Measurement of ^{57}Fe Nucleus using Mössbauer Spectroscopy.

Yichao Yu*
MIT Department of Physics
(Dated: March 16, 2013)

The Mössbauer spectroscopy is a technique for recoil-free measurement of nucleus gamma ray absorption spectrum in solid based on the Mössbauer effect. Because of the high resolution of the technique (10^{12}), it can be used to measure the tiny shift and splitting of nucleus energy levels when interacting with the environment. In this experiment, the Mössbauer spectrum was measured for ^{57}Fe atom for a variety of substance and different effects on the nucleus energy levels were observed.

Introduction

The nuclear resonance absorption was predicted in the late 1920's[1]. The idea was that the γ-ray emitted during a state transition from an excited state to ground state of a nucleus should be absorbed by another same nucleus in the exact reverse state transition. Although the same phenomenon was already be observed in atom radiation, the nuclear resonance absorption was not seen in experiment in the next 30 years due to the recoil Doppler shift for atoms in the gas state. The Mössbauer effect, discovered in 1958, provides a solution of the problem by elimiating the recoil. Combining with a precise frequency scanning using Doppler effect as well as the narrow linewidth of nuclear radiation, Mössbauer spectroscopy was invented to measure the spectrum of nucleus energy spectrum at a high resolution.

In this experiment, we measured the Mössbauer absorption spectrum of ^{57}Fe $14.4keV$ γ-ray in different substance including Fe, Fe_2O_3, $FeSO_4$, $Fe_2(SO_4)_3$, $Na_4Fe(CN)_6$, and stainless steel. A variety of effect that can shift or split the energy levels of the ^{57}Fe nucleus was observed including isomer shift, quadrupole splitting, zeeman effect and temperature shift.

1. THEORY.

1.1. Mössbauer spectroscopy.

The recoil velocity and the Doppler shift caused by that are given by,

$$v_{recoil} = \frac{E}{2mc}$$
$$\frac{\Delta E_{recoil}}{E} = \frac{E}{2mc^2}$$

where E is the original radiation energy, and m is the mass of the nucleus. For the $14.4keV$ radiation used in this experiment and free atom in the gas, the relative recoil shift is $2.8{\cdot}10^{-7}$, 5 orders of magnitude greater than the relative natural linewidth of the radiation 10^{-12}. In order to elimiate the recoil effect, Mössbauer embed the atom into a solid and therefore increase the mass in the denominator to an effective mass equal the the mass of the whole solid. Since the whole solid is about 10^{20} times heavier than the nucleus, the recoil shift is negligible.

By moving the source at a speed of the order $1cm \cdot s^{-1}$ under control, we are able to scan the energy of the γ-ray by $10^{10} - 10^{11}$ and measure the absorption spectrum of the target material precisely in this small energy range.

1.2. Shift and Splitting of energy levels.

In this experiment, we are looking for several effects that can either shift or split the energy levels of a ^{57}Fe nucleus.

1.2.1. Isomer shift

This effect is caused by the non-zero electron density at the nucleus. Since the radius of the excited and ground state of the nucleus are slightly different, the energy shifts are also different for the two states and therefore also shift the energy of the radiation. The energy shift is given by,

$$\delta = C\delta R|\psi(0)|^2$$

where δR is the difference of the two radius, $|\psi(0)|^2$ is the electron density at the nucleus, and C is a constant. Since the isomer shift exists for all samples, what we are going to observe in the experiment is a relative difference between the shift for different sample.

1.2.2. Zeeman effect

The excited state of the ^{57}Fe nucleus has a total angular momentum $I = \frac{3}{2}$ and the ground state has a total angular momentum $I = \frac{1}{2}$. Therefore, when there is a magnetic field at the nucleus generated by other electrons and atoms in the sample, the zeeman effect will split the excited and the ground states into 4 and 2 different energy levels respectively generating γ radiation of 6 possible energies as shown in figure 1.

*Electronic address: yuyichao@mit.edu; URL: http://yyc-arch.org/

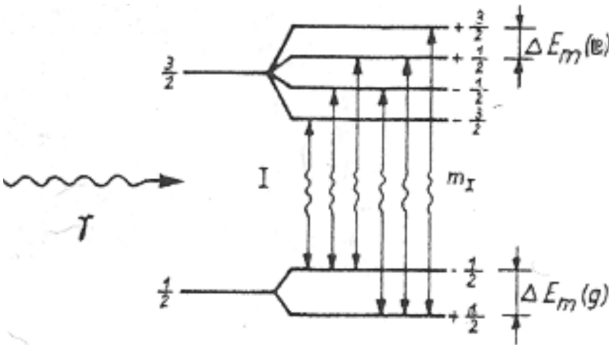

FIG. 1: Zeeman effect.

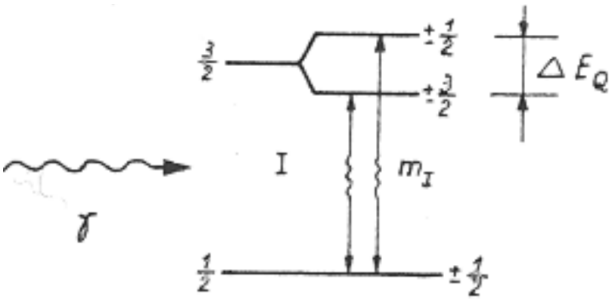

FIG. 2: Quadrapole Splitting.

The splitting and the energy correction of each levels are given by,

$$\begin{aligned}\Delta E_I =& g_I \mu_N B \\ E_I =& g_I m_I \mu_N B\end{aligned}$$

where g_I is the g-factor, μ_N is the nuclear magneton, m_I is the angular momentum projection quantum number, and B is the magnetic field.

1.2.3. Quadrapole Splitting

This effect is caused by the interaction between nuclear quadrapole moment and the inhomogeneity of the electric field. This correction to the energy levels is given by,

$$\Delta E_{quad} = \frac{qe^2Q}{4I(2I-1)}\left[3m_I^2 - I(I+1)\right]$$

where q is the guadiant of the field, Q the quadrapole moment. For the $I = \frac{1}{2}$ ground state $\Delta E_{quad} = 0$, whereas for the $I = \frac{3}{2}$ excited state (Figure 2),

$$\Delta E_{quad} = \begin{cases} \frac{qe^2Q}{4} & m_I = \pm\frac{1}{2} \\ -\frac{qe^2Q}{4} & m_I = \pm\frac{3}{2} \end{cases}$$

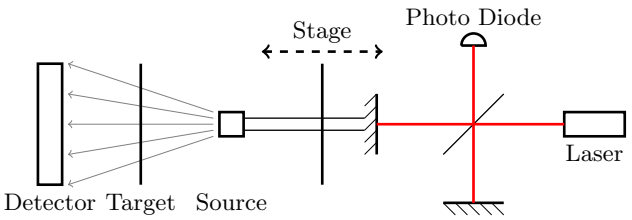

FIG. 3: Apparatus.

1.2.4. Temperature shift

This is a small effect caused by the relativistic time dilation caused by the random heat motion of the nucleus. The shift is given by,

$$\frac{\delta}{E} = \frac{\langle v^2 \rangle}{2c^2} = \frac{\langle E_k \rangle}{mc^2}$$

where $\langle v^2 \rangle$ is the averge speed square and $\langle E_k \rangle$ is the average kinetic energy of the nucleus.

1.2.5. Combination of multiple effects

Multiple effects can exist in the same sample and at most 6 absorption peaks can be observed. The energy shifts of these peaks are (temperature effect is ignored since it is small compare to other effects and will not change unless the temperature of the sample changes dramatically),

$$\begin{aligned}\Delta E_1 =& \varepsilon - \frac{\delta}{2} - \frac{3}{2}\Delta_1 - \frac{1}{2}\Delta_0 \\ \Delta E_2 =& \varepsilon + \frac{\delta}{2} - \frac{1}{2}\Delta_1 - \frac{1}{2}\Delta_0 \\ \Delta E_3 =& \varepsilon + \frac{\delta}{2} + \frac{1}{2}\Delta_1 - \frac{1}{2}\Delta_0 \\ \Delta E_4 =& \varepsilon + \frac{\delta}{2} - \frac{1}{2}\Delta_1 + \frac{1}{2}\Delta_0 \\ \Delta E_5 =& \varepsilon + \frac{\delta}{2} + \frac{1}{2}\Delta_1 + \frac{1}{2}\Delta_0 \\ \Delta E_6 =& \varepsilon - \frac{\delta}{2} + \frac{3}{2}\Delta_1 + \frac{1}{2}\Delta_0\end{aligned}$$

where ε is the isomer shift, δ is the quadrapole splitting, Δ_1 is the Zeeman splitting for the excited state and Δ_0 is the Zeeman splitting for the ground state.

2. APPARATUS AND CALIBRATION

2.1. Apparatus

Figure 3 is a schematics of the apparatus used in this experiment. The source is attached on a stage that can be moved back and forth in cycles under control of the

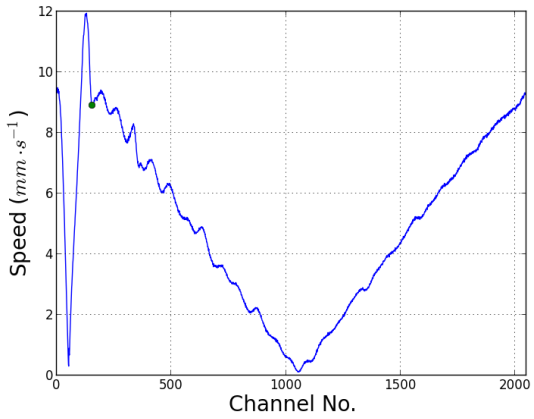

FIG. 4: Measurement of stage speed in each cycle. Each channel number in the horizontal axis corresponds to a certain time point in each scanning cycle.

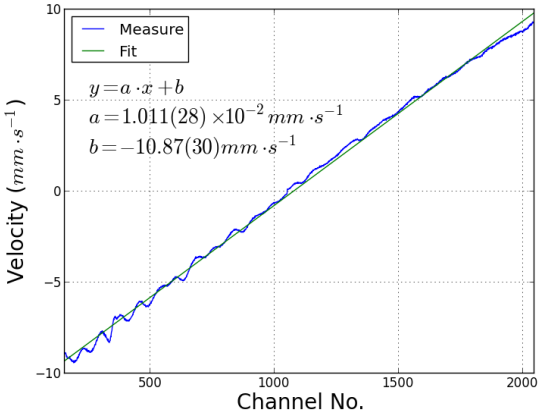

FIG. 5: Calibration fitting of velocity.

computer. A detector will measure the counting rate of radiation after absorbed by the target sample as a function of time in each scanning cycle and also send the data back to the computer.

2.2. Calibration of velocity using Michelson interferometer.

A Michelson interferometer with one mirror attached to the moving stage is used to calibrate the moving velocity of the stage (right half of figure 3). By measuring the power using the photo diode, the speed of the stage is,

$$|v| = 2f\lambda$$

where f is the frequency of the laser power and $\lambda = 632.8nm$ is the wavelength of the He-Ne laser used in the interferometer.

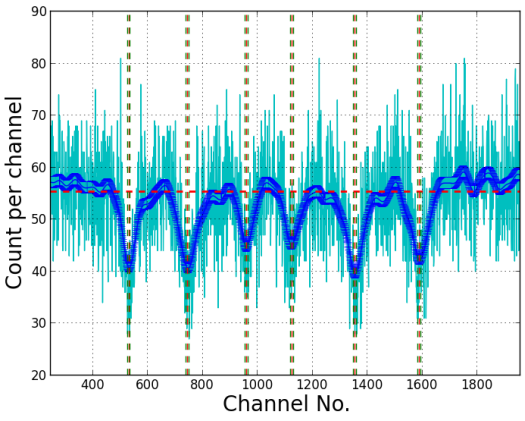

(a)Fe

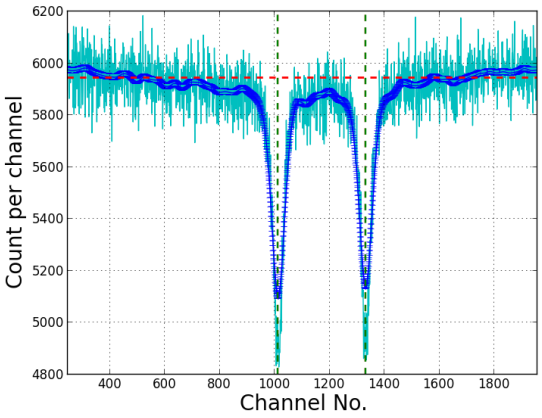

(b)$FeSO_4$

FIG. 6: Measured absorption spectrum of (a) Fe and (b) $FeSO_4$ samples. The light blue curves are the original data, the dark blue curves are the data after being smoothed. The vertical lines shows the position of peaks and the horizontal lines is an estimation of the total radiation level (without absorption of the target).

Figure 4 shows the relation between the speed of the stage and the time in each cycle (which is shown as channel numbers). After removing the first part where the velocity is changing rapidly and flip the sign for the region where the velocity is negetive, the calibration line was obtained by fitting a straight line to the data, as shown in figure 5.

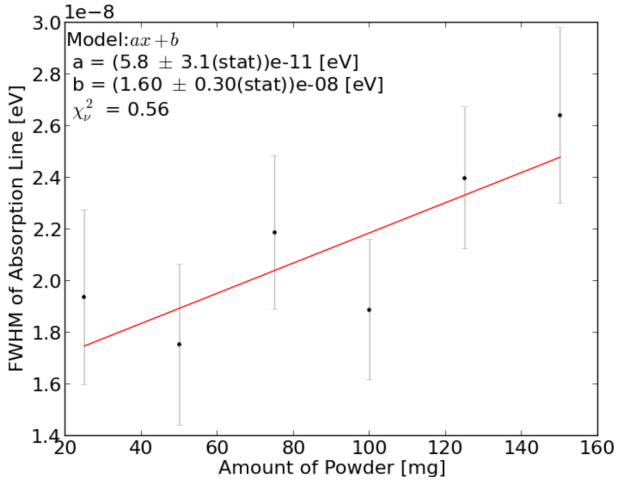

FIG. 7: FWHM (2Γ) of absorption peaks for different amount of $Na_4Fe(CN)_6$ samples.

3. MEASUREMENT OF DIFFERENT SAMPLES

3.1. Fe, Fe_2O_3, $FeSO_4$ and $Fe_2(SO_4)_3$

3.2. Measurement of linewidth using $Na_4Fe(CN)_6$ samples.

3.3. Measurement of temperature shift using stainless steel sample.

4. CONCLUSION

[1] W. Kuhn., Phil. Mag. pp. 625–636 (1929).

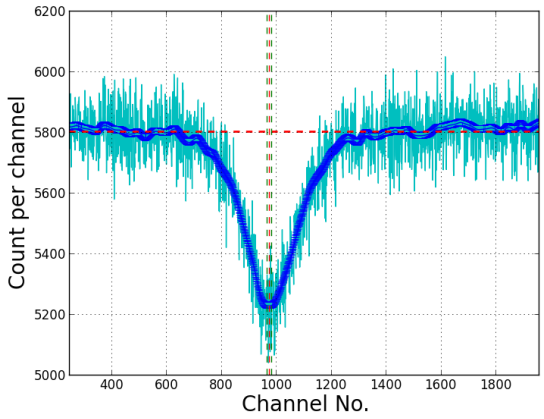

(a)21°C

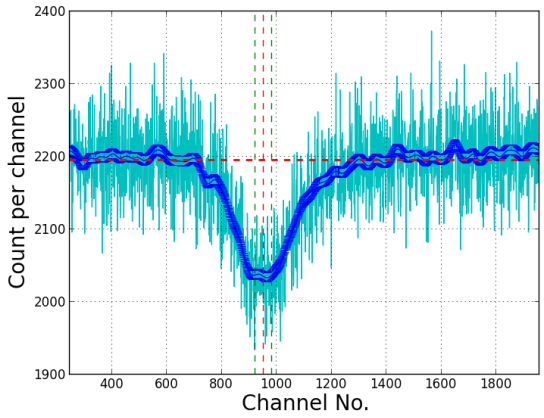

(b)130°C

FIG. 8: Measured absorption spectrum of stainless steel sample at (a) 21°C and (b) 130°C. The red verticle lines show the position of the peak and the green verticle line shows the uncertainty of the position. The uncertainty is magnified by a factor of 4 in order to be seen clearly on the plot.